NASA Technical Paper 1318

A High-Pressure Premixed Flat-Flame Burner for Chemical Process Studies

Irvin M. Miller

DECEMBER 1978

NASA

NASA Technical Paper 1318

A High-Pressure Premixed Flat-Flame Burner for Chemical Process Studies

Irvin M. Miller
Langley Research Center
Hampton, Virginia

National Aeronautics
and Space Administration

**Scientific and Technical
Information Office**

1978

SUMMARY

A premixed flat-flame burner was designed and tested for the purpose of studying chemical processes at high pressure, with the specific goal of studying pollutant formation in hydrocarbon flames. Successful operation of the burner was obtained with methane-air mixtures at equivalence ratios of 0.7, 0.9, and 1.1 and at pressures of 1.1, 5, 10, and 20 atm.

At each of the 12 pressure—equivalence-ratio combinations, the range of flame stability was determined as a function of reactant velocity. This velocity is defined in the present study as the average velocity of the reactant gas mixture in the burner mixing chamber. For each of the three equivalence ratios, the upper stability limit generally decreased with increasing pressure. As expected for an equivalence ratio of 0.9, the lower stability limit corresponds closely to the lower ignition limit for the same equivalence ratio.

To determine the maximum size of the thermocouple probe required for good spatial resolution in flames, flame zone thicknesses and flame heights were measured from color photographs. Flame height is the distance between the top of the burner and the bottom of the flame zone. Flame heights ranged from 0.16 to 0.85 mm, and flame zone thicknesses varied from 0.3 to 1.2 mm. These results show that thermocouple probes should be about 0.03 mm or smaller for good spatial resolution of the flame.

INTRODUCTION

The premixed flat-flame burner has been used for many years by many investigators to study flames in order to obtain a better understanding of combustion processes. The burner consists of either a bundle of small parallel channels or a fine porous metal disk contained at the end of a cylindrical chamber. A reactant gas mixture of fuel and oxidant flows upward through the fine passages at the top of the burner, represented by the porous disk in figure 1, and emerges in a uniform velocity distribution across the upper surface of the burner. Ignition of the gas mixture produces a flat flame across and close to the burner. The burner is usually cooled at the circumference, and is designed to operate over a wide range of stream velocities.

In the study of combustion processes, the premixed flame is often preferred over a diffusion flame (one in which the oxidant and fuel interdiffuse and burn at an interface). A premixed flame has a considerably simpler structure, and the rate of combustion is governed by chemical rate processes. In a diffusion flame, the rate of combustion is governed by both chemical rate and diffusion processes. Hence, many chemical kinetic studies have been made with premixed flames and especially with premixed flat flames. The flat flame is also preferred because flame properties, such as temperature and composition, are uniform in each plane parallel to the burner surface. Because of this uniform temperature property, flame temperature measurements made by thermocouple

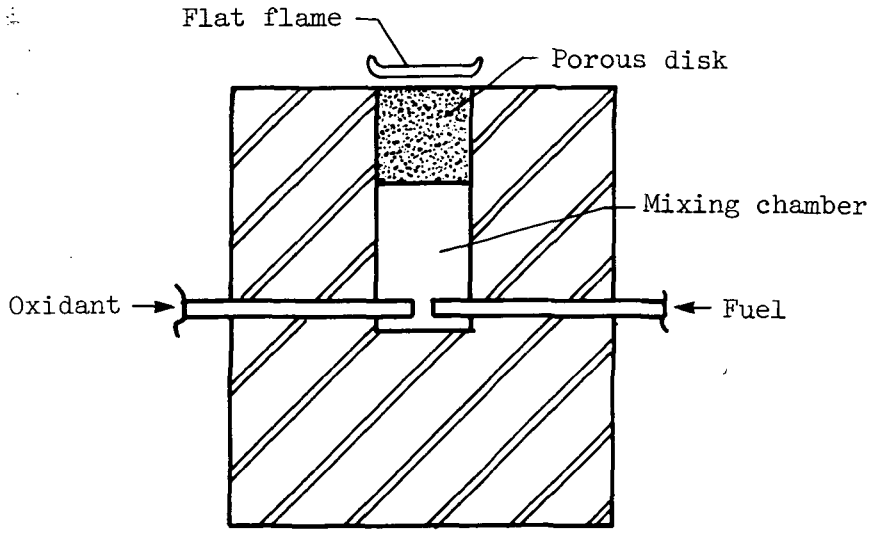

Figure 1.- Premixed flat-flame burner.

probes in these flames often do not require corrections for conduction errors, since the probes can usually be oriented in an isothermal plane of the flame. Since the properties of a premixed flat flame vary in one direction only, this flame is also called a one-dimensional flame.

There are at least two particular disadvantages to the study of premixed flames at high pressure. One is the danger of flashback, which is the upstream propagation of the flame through the burner to the gas mixture. This phenomenon usually occurs when the stream velocity instantly becomes smaller than the flame velocity, as when the reactant flow is suddenly interrupted or stopped. Under initial high-pressure conditions, the danger of flashback can cause a very high-pressure deflagration in the burner mixing chamber. There is also the danger of a detonation resulting therefrom, as reported by Edse in reference 1. Because of these hazards, only a limited number of high-pressure studies using a premixed flame have been made. These studies include soot formation and burning velocity by Diederichsen and Wolfhard (refs. 2 and 3), soot formation by Macfarlane, Holderness, and Whitcher (ref. 4), and burning velocity by Edse (ref. 1) and Strauss and Edse (ref. 5). A recent study was made by Heberling (ref. 6) of flat flames at pressures from 1 to 18 atm involving measurements of nitric oxide concentrations and flame temperatures. The second disadvantage is that the reaction zone in the flame decreases in thickness with increasing pressure. This makes it increasingly difficult to probe and sample this zone with good resolution.

In spite of these difficulties, the study of high-pressure premixed flat flames is needed to obtain a better understanding of combustion processes at high pressure. For instance, such studies might be concerned with determining the governing chemical mechanisms that control the rate of formation of pollutants, such as nitrogen oxides, sulfur dioxide, and soot. Data on such premixed flames can be useful in helping to formulate combustion models for predicting the formation rate of pollutants in practical combustion systems. To implement such a study, a burner described in this report was designed to extend the work

initiated by Miller and Maahs (ref. 7), which involved pollutant formation in high-pressure diffusion flames.

The purpose of the present study is to design, test, and determine the stable operating range of a premixed flat-flame burner at high pressures as well as the flame dimensions on such a burner, i.e., flame height (preheat zone) and flame thickness (reaction zone). The extent of the stability range and flame dimensions will determine the suitability of the burner for the study of chemical processes in flames at high pressure. For this purpose, fuel-lean and near-stoichiometric mixtures of methane and air were burned at pressures from 1.1 to 20 atm.

SYMBOLS

A_b	projected cross-sectional area of porous disk in burner, 1.27 cm^2
C	constant, $(mole\text{-}sec^2)/(g\text{-}cm^6\text{-}K)$
F( )	mathematical function of ( )
f	friction factor
K	constant, $moles/cm^4$
L	depth of a porous medium, cm
M	molecular weight, g/mole
N_{Re}	Reynolds number
n	number of moles
p	pressure, atm (1 atm = 101.3 kPa)
p_b	absolute pressure in burner mixing chamber, atm
$\bar{p}$	average pressure in a porous medium, atm
Δp	pressure drop across porous disk in burner, atm
q_d	quenching diameter, mm
q_ℓ	quenching length, mm
R	universal gas constant, $(cm^3\text{-}atm)/(mole\text{-}K)$
S	cross-sectional area of a porous medium, cm^2
s_p	surface area of a particle, cm^2

T	absolute temperature, K
T_b	absolute temperature in burner mixing chamber, K
$\bar{T}$	average absolute temperature in a porous medium, K
u_b	reactant velocity, cm/sec
$\bar{u}$	average velocity of fluid, cm/sec
V	volume, cm^3
$\dot{V}$	volumetric flow rate, cm^3/sec
$\dot{V}_b$	volumetric flow rate in burner mixing chamber, cm^3/sec
v_p	volume of particle, cm^3
α	pressure exponent, an empirical constant
β	temperature exponent, an empirical constant
ε	void fraction or porosity
$\bar{\mu}$	average viscosity of a fluid in a porous medium, g/(sec-cm)
ρ	density of fluid, g/cm^3
ϕ	equivalence ratio

Subscripts:

a	air
f	fuel
ref	reference value
s	standard conditions of temperature and pressure, 293 K and 1 atm
1	upstream of porous medium
2	downstream of porous medium

DESIGN CONCEPT AND BURNER CONFIGURATION

The stabilization of a flame in a flat-flame burner is based on the fact that flame velocity, i.e., the velocity at which a flame propagates in a reactant gas mixture, varies with flame temperature (ref. 8). Thus, as the flame propagates upstream to the burner surface, it loses an increasing amount of heat to the burner, causing the flame temperature to drop until the flame

velocity is equal to the stream velocity of the unburned mixture upstream of the flame. Then the flat flame remains at a fixed distance close to the burner surface. By increasing the stream velocity, the velocity of the flame and its temperature must increase, which results in the flame taking a position farther away from the burner. By continually increasing the stream velocity, the flame can approach the adiabatic flame temperature and hence the adiabatic flame velocity. To more efficiently extract heat from the flame in order to obtain a more stable flame, the porous disk in the burner is usually radially cooled. The simplest means of cooling is a heat sink as shown in figure 2. Because of its simplicity, this method of heat removal was chosen for the present burner.

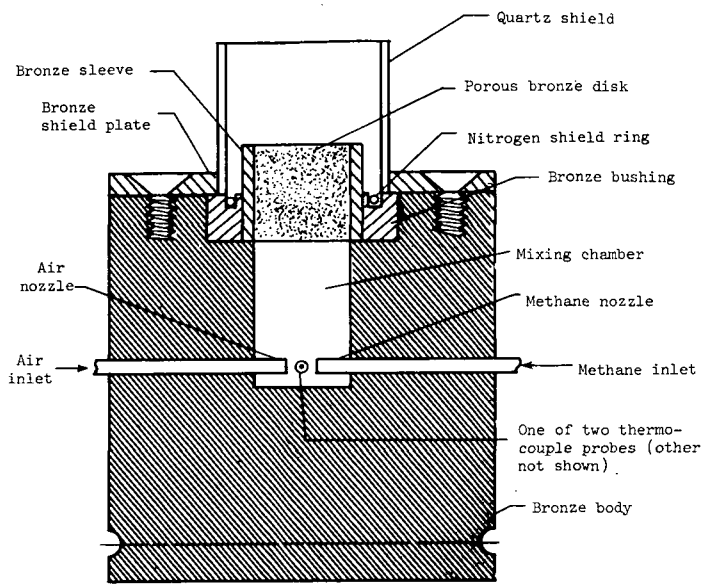

Figure 2.- High-pressure flat-flame burner. Full scale.

As previously noted, the hazards of using a premixed burner operating at initial high-pressure conditions are flashback, which can cause a very high-pressure deflagration in the mixing chamber, and possible detonation, where the peak pressure is twice that of a deflagration for the same initial conditions (ref. 9). Flashback can be minimized by keeping the dimension of the narrow channels in the burner plate below the quenching length q_ℓ. This length is defined as the smallest separation between two parallel plates which will allow a flame to pass.

A study of the literature revealed that quenching length depends on pressure, temperature, geometry of quenching surface (such as a tube or slit), and reactant composition (ref. 10). Friedman and Johnston (refs. 11 and 12) studied quenching length with a slit burner at various pressures and temperatures for a number of hydrocarbon-air mixtures and found the following relation:

$$q_\ell \propto \frac{1}{p^{\alpha} T^{\beta}}$$

where p is absolute pressure, T is absolute temperature, and α and β are empirical constants. Their study showed that the minimum quenching length occurred at near-stoichiometric fuel-air ratios (110 percent of stoichiometric). Friedman and Johnston's value of α for several hydrocarbon-air mixtures (propane, benzene, n-heptane, and isooctane) varied from 0.87 to 0.92 for a pressure range of 0.08 to 4 atm. Their value of β for the same near-stoichiometric propane-air flames was 0.5, where temperatures were varied from 300 to 558 K. Nair and Gupta (ref. 13) determined quenching lengths in a closed spherical combustion bomb for stoichiometric butane-air mixtures from 4.2 to 30 atm; from their plotted data, α is 0.79. In a similar study by Green and Agnew (ref. 14), for slightly rich propane-air mixtures from 2 to 60 atm, α is 0.64. The values of α from the last two studies are lower than those found by Friedman and Johnston (refs. 11 and 12); however, for a safer design that would specify a smaller quenching distance, the larger value of $\alpha = 0.9$ was assumed along with the value of $\beta = 0.5$.

If one assumes that the relation for quenching length also applies to the diameter of a tube, then the quenching diameter q_d, the smallest diameter that will allow a flame to pass, will have the same relationship to pressure and temperature, or

$$q_d \propto \frac{1}{p^{\alpha} T^{\beta}} \tag{1}$$

This expression can also be written as

$$\frac{q_d}{q_{d,ref}} = \left(\frac{p_{ref}}{p}\right)^{\alpha} \left(\frac{T_{ref}}{T}\right)^{\beta} \tag{2}$$

where $q_{d,ref}$ is the quenching diameter for a given reactant composition at a reference pressure p_{ref} and reference temperature T_{ref}. The reactant composition for this study will be various ratios of methane to air. The methane-air ratio that gives the smallest quenching diameter should be the one that is slightly richer than the stoichiometric mixture, as was the case for the smallest quenching length of other hydrocarbon-air mixtures noted previously. Von Elbe and Lewis (ref. 15) list an experimentally determined quenching diameter of 0.335 cm for a methane-oxygen-nitrogen mixture at atmospheric pressure and room temperature that closely approximates a methane-air flame that is slightly richer than stoichiometric. If these values of quenching diameter, pressure, and temperature are used in equation (2), and if, for conservatively safe operating conditions at 20 atm, $p = 50$ atm and $T = 673$ K are used, then $q_d = 0.066$ mm. Thus, if a porous metal disk is selected with the largest pore size less than 0.066 mm, the possibility of flashback should be small. For the burner of this study, a porous bronze disk with a mean pore size of 0.025 mm was selected. This disk had a very closely packed structure of sintered spherical particles 0.13 mm in diameter.

Since equation (2) is based on limited experimental data, the mean pore size selected for the present burner may not prevent flashback, which could possibly even result in a detonation. Lewis and Von Elbe (ref. 16) note that detonation can occur within 60 tube diameters when a flammable mixture is ignited at one end of a long tube. They attribute this to the onset of turbulence, a condition which usually occurs between 50 and 100 tube diameters from the inlet. However, turbulence initiators, such as obstructions, can reduce the 60-diameter length to 5 diameters. Therefore, for a conservative design, the length of the mixing chamber in the present burner was made 1.5 diameters. In addition, two thermocouples were located in the mixing chamber (see fig. 2), and the signals from these sensors were used to close a solenoid valve in the fuel line in the event of flashback.

With the foregoing precautions taken in the design of the burner, namely, fine porous metal disk, short mixing chamber, and provision for instant fuel cutoff, the hazards of flashback and detonation are considered minimized. If either flashback or detonation does occur, the burner mixing chamber and porous disk should have the necessary mechanical strength to contain the pressures involved. The mixing chamber is made of bronze and has thick walls capable of holding pressures of several thousand atmospheres. The bronze porous disk, which has a diameter of 1.27 cm, is 1.27 cm thick, and has a composition of 90-percent copper and 10-percent tin, was estimated to be capable of withstanding at least 1000 atm.

It was noted previously that the premixed flat-flame burner is usually cooled at the circumference to allow the burner to operate over a wide range of reactant velocities. However, if the burner surface is not uniformly cooled, the flame cannot be stabilized as a flat flame. An analysis of the effect of burner diameter and thickness on the temperature and velocity uniformity of circumferentially cooled porous-disk burners was made by Kihara, Fox, and Kinoshita (ref. 17). Their study showed that in order for the reactant flow to approach a one-dimensional flow, the burner diameter should be made as small as possible. For this requirement, the small diameter of the porous disk was considered adequate. However, Pritchard, Edmondson, and Heap (ref. 18) have concluded that the burner diameter should be large to minimize diffusive effects at the edge of the flame. To minimize these effects, Spalding and Yumlu (ref. 19) used a mica shield around the flame, and similarly, for the present burner design, a cylindrical quartz shield (20-mm inside diameter by 16-mm height) was used.

To obtain as complete mixing as possible of the fuel and air flows entering the mixing chamber, the fuel and air nozzles were located so as to oppose each other as shown in figure 2. In addition, the circular orifice of the air nozzle was decreased in size from 1.52 mm to 1.02 mm to increase the velocity of the air jet and thus promote air turbulence a short distance from the point of discharge (ref. 20). Thus, with the air and fuel nozzles in opposition to one another, and with a turbulent air jet, good mixing of fuel and air is likely. Evidence for good mixing was seen in preliminary tests by the uniformly blue color of the flame for all mixture ratios.

The burner is provided with a nitrogen shield ring between the porous disk and the cylindrical quartz shield (see fig. 2) to sweep the inside of the shield with nitrogen and thus prevent condensation of water, which might occur at high pressures. The nitrogen shield was not used in this study since no condensation on the quartz shield was observed.

It was important to have a flame that closely approximated a one-dimensional flame. For this purpose, six porous bronze disks were tested. Each disk was 1.27 cm in diameter and 1.27 cm thick and had a mean pore diameter of 0.025 mm. Each disk was shrink-fitted into a bronze sleeve, and a special test burner (fig. 3) was designed. Methane and air flows were controlled by needle valves

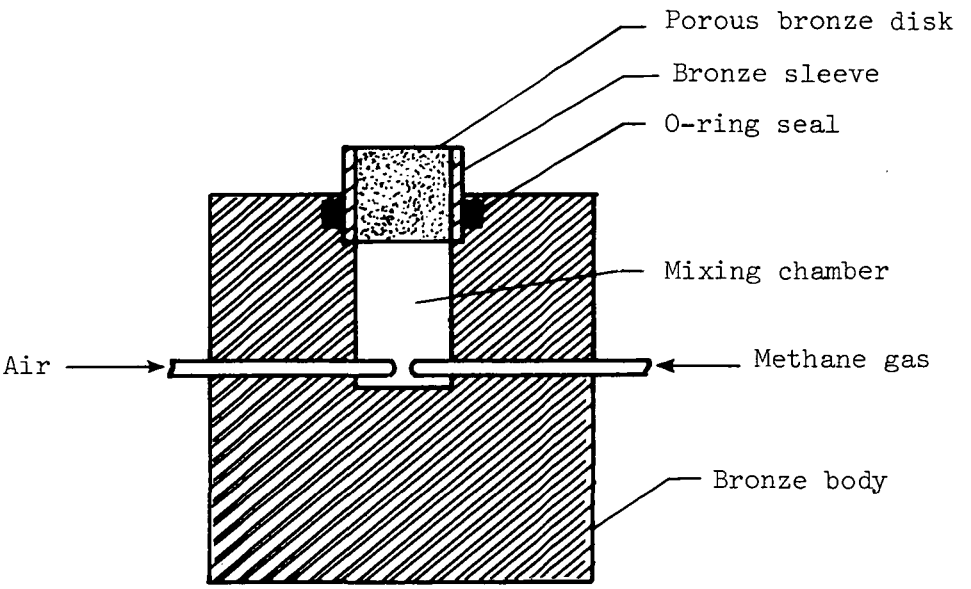

Figure 3.- Test burner. Full scale.

from pressure-regulated cylinders. Reactant velocity[1] was 22 cm/sec and the methane-air mixture was 30 percent richer than stoichiometric. A stirrup-type thermocouple of iridium/iridium—plus 40-percent rhodium was used to measure the temperature, and the burner was moved laterally on a micrometer-type motor-driven table. The thermocouple was located at the center of the burner and moved vertically to locate the maximum temperature, then a lateral traverse was made. Data from all six disks indicated a more uniform temperature profile for two of the six disks; i.e., a minimum of 7-percent deviation in measured thermocouple temperature between the center, 1640 K, and 1 mm from the edge, 1530 K. However, after one disk-sleeve assembly was selected and was shrink-fitted into the high-pressure burner and tested for flame uniformity in the same manner, a 17-percent deviation was found between the center, 1490 K, and 1 mm from the edge, 1255 K. The increased temperature deviation in the high-

[1]Reactant velocity is the average axial velocity of the reactant gas mixture in the burner mixing chamber.

pressure burner may be due to the cooling effect of the larger amount of metal surrounding the porous disk in the high-pressure burner, compared with the O-ring seal contact in the test burner. The measured temperature deviation is only approximate and is probably overstated due to the thermocouple conduction errors near the edge of the flame. In addition, the flame appeared flat and was curved upward only at the edges, as expected. Therefore, the high-pressure burner was considered acceptable for the present study.

THE HIGH-PRESSURE SYSTEM

The burner was installed in a high-pressure chamber which had been designed to study diffusion flames at pressures up to 50 atm. The overall system is described in reference 7. Briefly, it consists of a high-pressure chamber housing the burner, a heated total-sample collection system, back-pressure regulation to control chamber pressure (see fig. 4), and a flow-control system

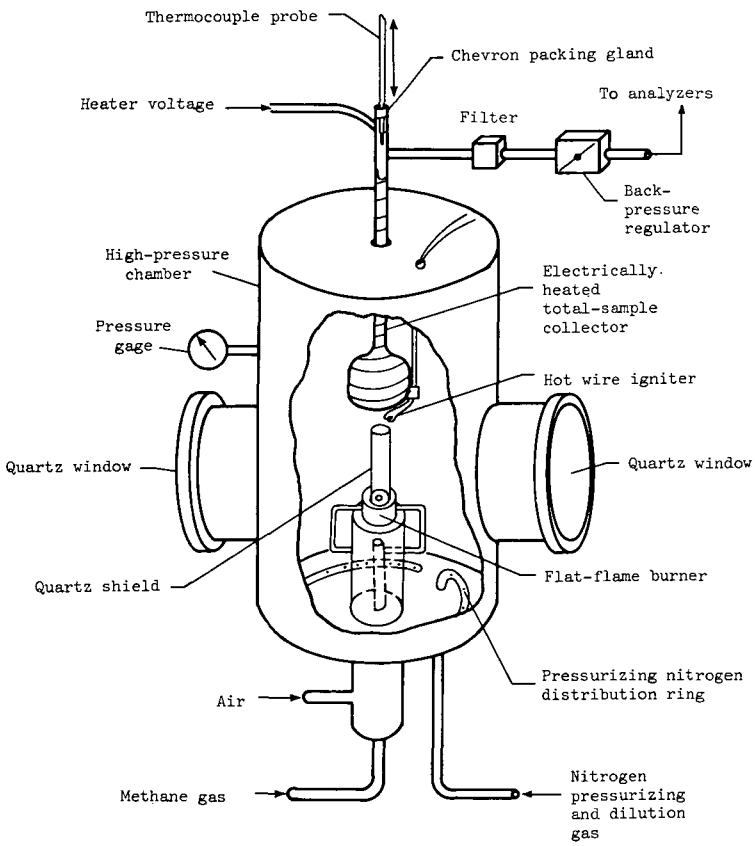

Figure 4.- Schematic diagram of burner and sample collection system.

which is not shown in the figure. The flow and pressure control system regulates the flow of air, gaseous fuel, and nitrogen-pressurizing gas. These flows are controlled by micrometer needle valves, the upstream pressure of

which is controlled by pressure regulators. The downstream, or chamber, pressure is controlled by a back-pressure regulator. Flow rates for methane and air are measured by calibrated linear thermal mass flowmeters that read flow rates at standard conditions of 1 atm and 293 K. Chamber pressure was measured by two separate Bourdon tube gages. The lower pressures of 1 and 5 atm were measured with a gage having a pressure range from 0 to 10.2 atm and an accuracy of 0.066 percent of full scale. The higher pressures of 10 and 20 atm were measured with a gage having a pressure range of 1 to 69 atm and an accuracy of 0.1 percent of full scale.

OPERATION

To obtain a premixed flat flame at a specified pressure, the pressure chamber was first pressurized with nitrogen gas (99.995 percent pure), and chamber pressure was set with the back-pressure regulator. When the desired chamber pressure was reached, air (99.995 percent pure) and methane (99.97 percent pure) flows were begun and adjusted to values corresponding to a desired reactant velocity and an equivalence ratio[2] of 0.90. (Equations for calculating the reactant velocity and equivalence ratio are developed in appendix A.) Electric heaters for the total sample collector and associated transfer lines were energized to prevent steam condensation. When the desired sample-line temperatures were reached, the hot-wire igniter above the cylindrical quartz shield (see fig. 4) was energized. If the flame failed to ignite at the set reactant velocity, as indicated by repeated flashback from the top to the bottom of the quartz shield, a higher reactant velocity was set, and ignition was again attempted until a flame stayed on the burner. Methane and air flow rates were then varied over a range of reactant velocities at this and two other equivalence ratios, 0.7 and 1.1.

Values of the equivalence ratio ϕ and the volumetric flow rate of the unburned gas mixture at standard conditions $\dot{V}_s$ were calculated as follows:

$$\phi = \frac{\dot{V}_{f,s} / \dot{V}_{a,s}}{0.105}$$

and

$$\dot{V}_s = \dot{V}_{f,s} + \dot{V}_{a,s}$$

where $\dot{V}_{f,s}$ and $\dot{V}_{a,s}$ are the measured volumetric flow rates of methane and air, respectively, at standard conditions, and 0.105 is the molar ratio of methane to air for a stoichiometric mixture. The reactant velocity u_b was calculated as follows:

---

[2]Equivalence ratio is the molar fuel-to-air ratio in the gas mixture divided by the molar fuel-to-air ratio for a stoichiometric gas mixture.

$$u_b = \frac{\dot{V}_b}{A_b}$$

where A_b is the projected cross-sectional area of the porous disk, which is the same as the cross-sectional area of the burner cavity, and $\dot{V}_b$ was calculated from equation (A6), which is

$$\dot{V}_b = \frac{p_s T_b}{p_b T_s} \dot{V}_s$$

where $\dot{V}_b$ is the volumetric flow rate of the methane-air mixture in the burner cavity, T_b and p_b are the absolute temperature and pressure, respectively, in the burner cavity, and T_s and p_s are the absolute temperature (293 K) and pressure (1 atm), respectively, at standard conditions. The value of p_b was not measured directly, but was determined from the relation

$$p_b = p + \Delta p$$

where Δp is the pressure drop across the porous disk. The magnitude of Δp was determined in separate tests at the end of this study in which Δp was plotted against flow rate through the burner. (See fig. 5.) Nitrogen was used in these studies because its viscosity closely approximates the viscosity of the methane-air mixture.

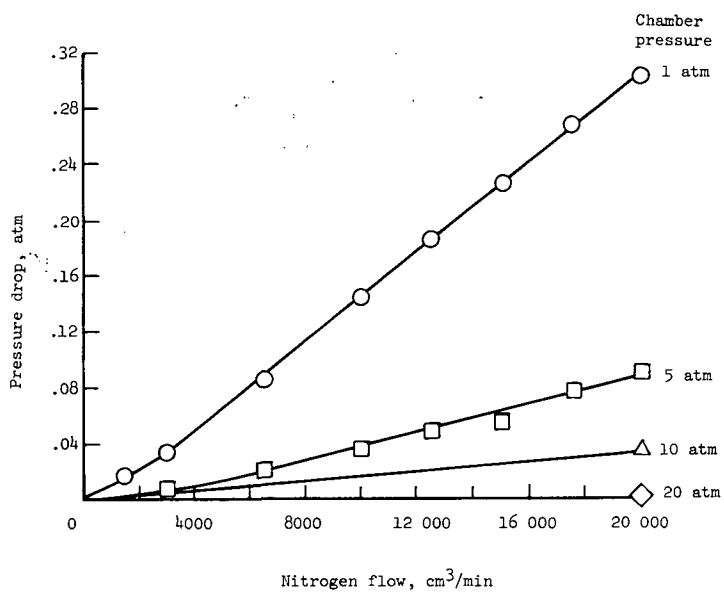

Figure 5.- Pressure drop across flat-flame burner versus nitrogen flow under standard conditions.

An estimate of the error in p_b, and hence in u_b, was made from an analysis presented in appendix B. In this analysis the nitrogen-flow—pressure-drop data were correlated by a friction-factor—Reynolds number equation for porous solids, the Kozeny-Carman equation (ref. 21). The resulting correlation was then used to estimate pressure drop for assumed average temperatures and reactant flow rates in the porous disk. The results of this analysis show that p_b could be understated by as much as 12 to 18 percent, depending upon an assumed average temperature in the porous disk of 400 K or 450 K. This means that the maximum values of u_b calculated in this study could be overstated by this amount.

RESULTS AND DISCUSSION

In figures 6, 7, and 8, the reactant velocity is plotted against pressure for equivalence ratios of 0.7, 0.9, and 1.1, respectively. Each figure shows the range of reactant velocity for a stable flame, hereinafter referred to as the stable range. In figures 7 and 8 a dashed line is drawn to represent the adiabatic flame-velocity, or burning-velocity, data of Diederichsen and Wolfhard (ref. 3) for methane-air mixtures in a Bunsen burner. No comparable data are available for figure 6. Although there is approximate agreement between these

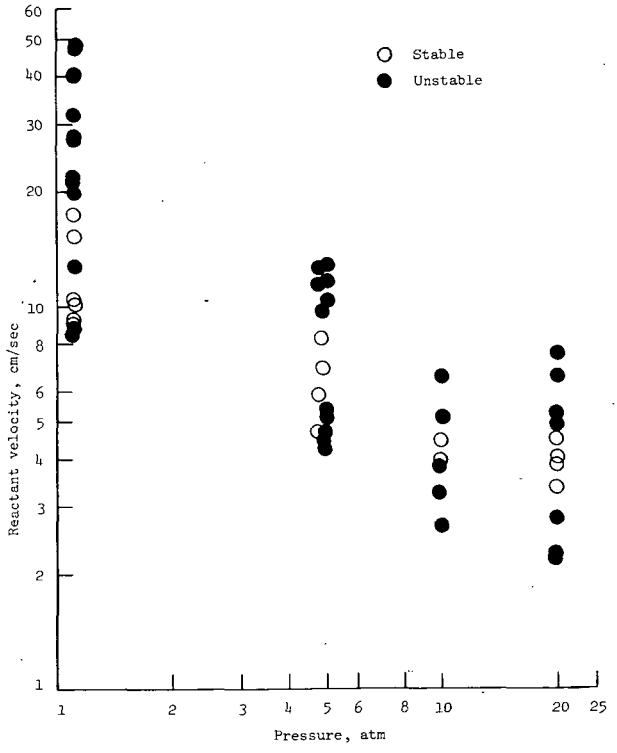

Figure 6.- Stable and unstable regions of a methane-air premixed flat flame at various pressures. $\phi = 0.7$.

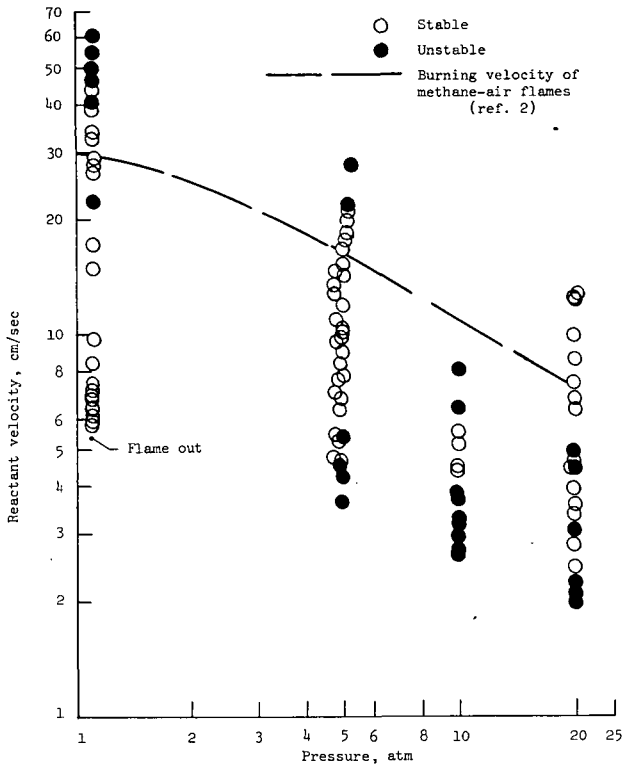

Figure 7.- Stable and unstable regions of a methane-air premixed flat flame at various pressures. ϕ = 0.9.

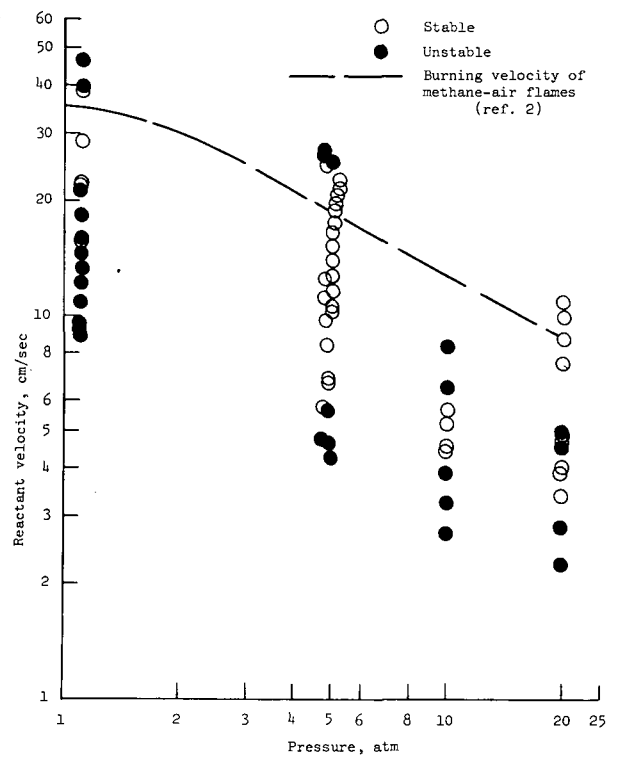

Figure 8.- Stable and unstable regions of a methane-air premixed flat flame at various pressures. ϕ = 1.1.

curves and the upper limit of the stable range, the deviations are not unexpected; in a flat-flame burner the flame becomes unstable at reactant velocities well below the burning velocity (see ref. 22), whereas in the Bunsen burner the reactant velocities closely approach that velocity. In addition, the Bunsen burner method for measuring burning velocities is subject to considerable error. For example, according to Botha and Spalding (ref. 22) the burning velocity of stoichiometric propane-air mixtures measured by this method under comparable conditions showed a variation among seven workers of from 33 to 44 cm/sec. All of these data involved measurements that were made on a curved flame front, so that the definition of the area of the flame was uncertain and subject to error.

The stable ranges for the three equivalence ratios ϕ have some features in common, but there are also marked differences between them. The general trend for all three equivalence ratios from 1.1 to 20 atm is a decrease in the upper limit of the stable range, which is in agreement with the work of Diederichsen and Wolfhard (ref. 3) for similar methane-air mixtures in a Bunsen burner. The stable range narrows considerably at 10 atm for all three equivalence ratios. For $\phi = 0.7$ (see fig. 6), the stable ranges are small for all four pressure levels. For $\phi = 0.9$ and 1.1 (see figs. 7 and 8), the stable ranges are similar, except at 1.1 atm, where the range is very small for $\phi = 1.1$ but quite broad for $\phi = 0.9$. Due to flow measurement limitations, no upper limit was found in the stable range for $p = 20$ atm and $\phi = 0.9$ and 1.1, as shown in figures 7 and 8.

Just below the lower limit of the stable range for $\phi = 0.9$ and $p = 1.1$ atm is flameout. (See fig. 7.) The lower limits of the stable range for $\phi = 0.9$ in figure 7 are in fair agreement with the ignition curve in figure 9 generated for $\phi = 0.9$. Although no attempt was made to investigate the upper bound for ignition, it is interesting to note that the data plotted in figure 9 for $p = 1.1$ atm show an upper ignition limit in fair agreement with the upper limit of the stable range in figure 7 for $\phi = 0.9$ and $p = 1.1$ atm.

In a study of the literature, Gaydon and Wolfhard (ref. 8) found that for hot flames, such as those with oxygen or acetylene-air, the burning velocity varied little with pressure; for cooler flames with air they found a marked negative dependence of burning velocity upon pressure. The upper and lower bounds of the stable ranges in figures 6, 7, and 8 also show a marked negative dependence on pressure. The difference in burning velocity response between cooler and hotter flames is probably due to a difference in reaction rates taking place in each type of flame. However, no literature data are available to explain these phenomena. It is apparent that additional work needs to be done in this area.

The instabilities indicated in figures 6, 7, and 8 fall into four main categories: vibration, lifting, humps, and flame spikes. Vibration instabilities consist of slow or rapid vibrations of part or all of the flame front.

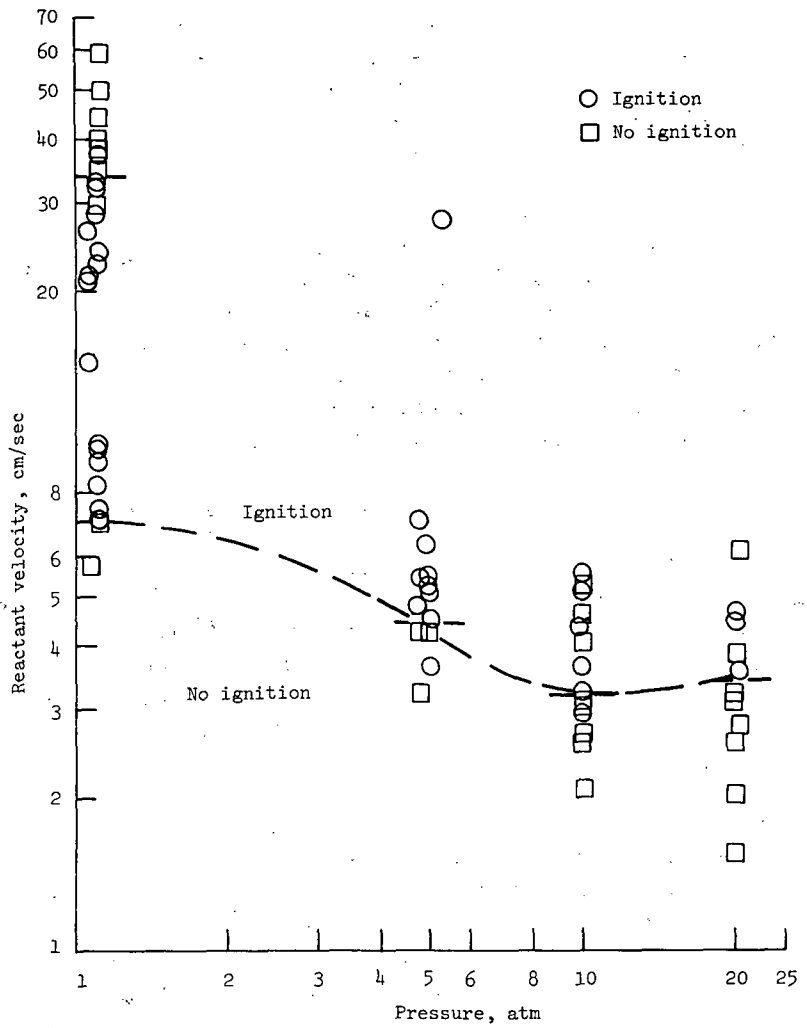

Figure 9.- Ignition conditions for a methane-air premixed flat flame. $\phi = 0.9$.

Lifting occurs when one side or edge of the flame front lifts away from the burner. Humps are bulges in the center of the flame front, often accompanied by lifting of one or both sides of the front. A flame spike is a narrow, pointed, orange-colored flame that appears near the edge of the flame front. Below the stable range, the instabilities are of either the vibration or lifting type. Above the stable range, the instabilities include all four types. The lifting instability observed above the stable range may be explained as follows. Under stable flame conditions, the reactant gas is cooled more at the periphery of the porous disk than at the center, which results in a lower viscosity and higher velocity of the gas in that region. For a flame to exist in

this higher velocity region, the flame front must curve upward in order that the normal component of the stream velocity be equal to the flame velocity. If the normal component of the stream velocity exceeds the flame velocity, the flame will lift away from the burner until the normal component of the stream velocity is again equal to the flame velocity. This would explain the lifting instability observed above the stable range. The humps or bulges in the center of the flame front are not the same as the cellular structure type of instability described by Botha and Spalding (ref. 22) and others; the reason for the observed instability is not known. Luminous flame spikes appeared near the edge of the flame front at 10 and 20 atm for $\phi = 0.9$ and 1.1, and at 5 atm for $\phi = 0.7$. The fact that these spikes appeared near the edge of the flame front is suggestive of a low-resistance path for the fuel-air mixture. However, it is not understood why no flame spikes were seen at 10 and 20 atm for $\phi = 0.7$. Lifting instabilities below the stable range could be the so-called "tilted" flames described by Lewis and Von Elbe (ref. 16).

The foregoing results describe reactant velocity operating ranges as a function of pressure for stable flat flames of methane-air mixtures for the burner designed and used in this study. These results may not be applicable to another burner having a porous disk of a different size. For example, a larger diameter or thinner disk would be expected to have a greater temperature and velocity deviation between the center and edge of the disk, as demonstrated by the analytical study of Kihara, Fox, and Kinoshita (ref. 17). These deviations could produce smaller stability regions than those reported in this study.

An important parameter in flame chemistry is flame temperature, which is usually measured by a thermocouple probe. Although flame temperature measurement was not intended in the present study, it was considered desirable to obtain flame dimensions so that thermocouple probes could be designed for future studies. Therefore, color photographs were taken to determine the flame zone thickness and height of the flame above the burner. For this purpose, a 35-mm, single-lens-reflex camera was used with color negative film. The camera was fitted with a reflective lens that had a focal length of 200 mm and an aperture of f/2.8. The camera was modified to take a double exposure: the first exposure for the flame and the second for a silhouette of the top surface of the shield plate. (See fig. 2.) For this second exposure, a back-lighted knife edge was focused on the shield-plate surface so that a thin beam of light illuminated that surface but not the surface of the porous disk. The shield-plate surface was used as a measurement reference to obtain the height of the flame zone above the porous disk. (The surface of the porous disk was not suitable as a measurement reference because preliminary photographs of the flame showed very little contrast between the burner surface and the dark background.) A scaling factor and height reference were obtained from a separate photograph showing the top of the shield plate and porous disk in silhouette. The diameter of the encased porous disk was known from a micrometer measurement. All measurements were made from color enlargements. (See fig. 10.)

Working pressure, 1 atm; reactant velocity, 7 cm/sec

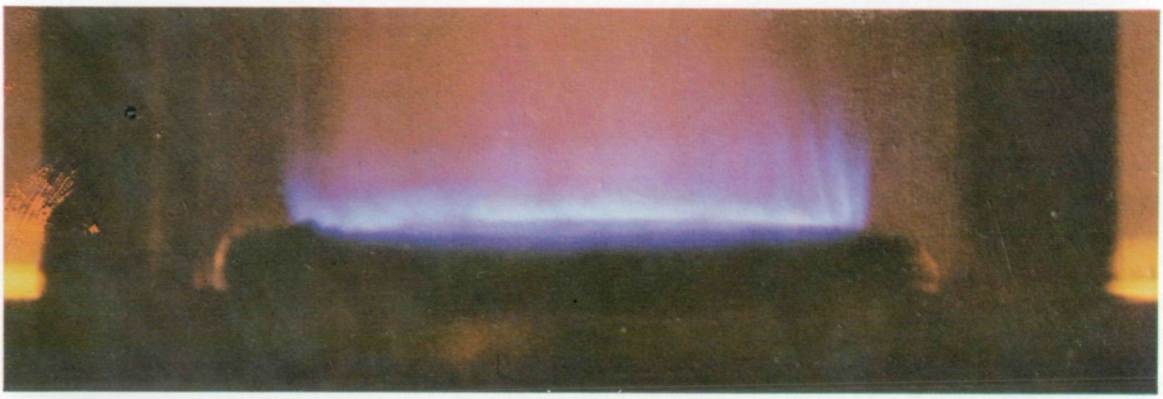

Working pressure, 20 atm; reactant velocity, 3 cm/sec

Burner silhouette

L-78-142

Figure 10.- Color photographs of methane-air premixed flat flames and burner silhouette. $\phi = 0.9$.

The data for flame zone thickness are plotted in figure 11 against reactant velocity. A separate plot is shown for each equivalence ratio. The plotted data are for stable flames and show that flame zone thickness varies from 0.3 mm at low velocities to 1.2 mm for high velocities. Note that the flame zone thickness for pressures of 10 and 20 atm is in the low range of 0.3 to 0.7 mm due to the low velocities associated with the higher pressures. For good spatial resolution, thermocouple probes should, in the author's opinion, have a diameter of about 0.1 to 0.2 of the flame zone thickness, or for these flames, about 0.05 mm. Figure 11 tends to give the impression that flame zone thickness is independent of pressure and equivalence ratio. However, data of Bonne, Grewer, and Wagner (ref. 23) show that the flame zone thickness for a methane-oxygen flat flame is inversely proportional to pressure between 2 and 20 torr (1 torr = 0.001316 atm) at constant mass flow rate. Accordingly, the flame zone thickness data of figure 11 were plotted against mass flow rate and cross-plotted against pressure to investigate the possibility of a real variation of flame zone thickness with pressure at constant mass flow rates. This

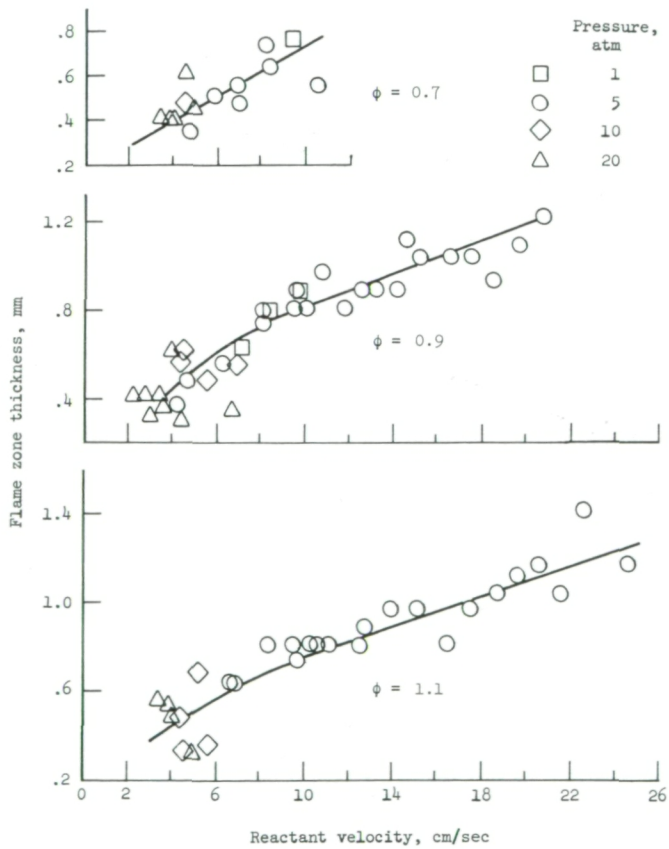

Figure 11.- Variation of flame zone thickness with reactant velocity.

is shown in figure 12. Although the data in this figure are limited, the trends are in general agreement with the data of Bonne, Grewer, and Wagner (ref. 23).

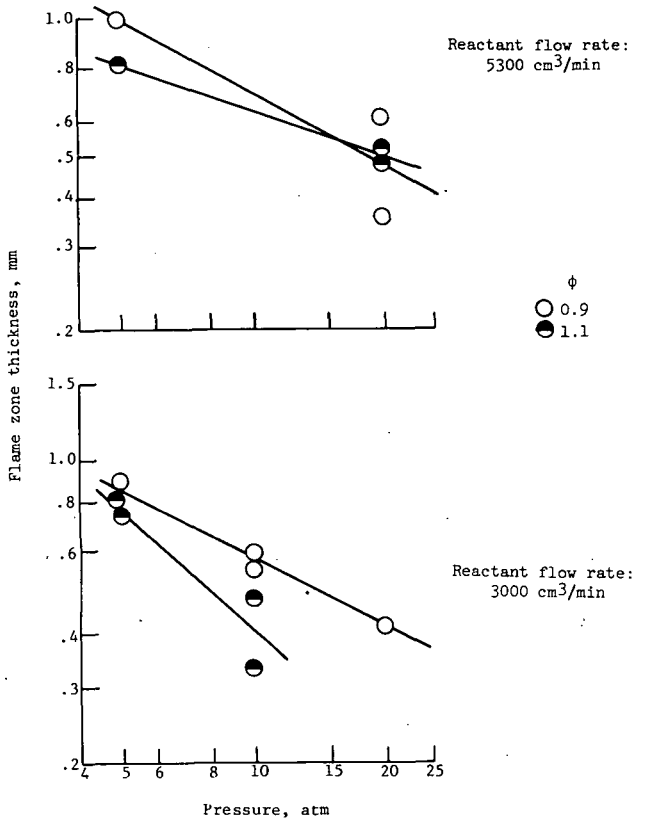

Figure 12.- Variation of flame zone thickness with pressure at constant mass flow rate under standard conditions.

The flame height was measured from the color enlargements as the distance from the top of the porous disk to the bottom of the flame zone. This distance corresponds to the preheat zone of the flame. These data are plotted against pressure in figure 13. The heights shown vary from 0.16 to 0.85 mm, which

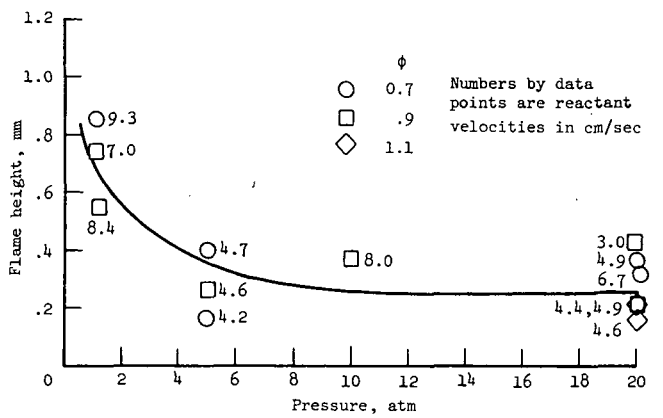

Figure 13.- Variation of flame height with pressure.

means that a thermocouple probe should be smaller than about 0.03 mm for probing the preheat zone adequately. The number shown beside each data point in figure 13 is the corresponding reactant velocity in cm/sec. Most of the data associated with low-reactant velocities have small flame heights, as expected.

CONCLUDING REMARKS

A premixed flat-flame burner was designed for the study of chemical processes during the high-pressure combustion of methane with the specific goal of studying pollutant formation in hydrocarbon flames. The burner was installed in an existing high-pressure facility and was operated successfully with methane-air mixtures at pressures of 1.1, 5, 10, and 20 atm and equivalence ratios of 0.7, 0.9, and 1.1.

Reactant velocity was used to indicate the range of flame stability. For a given equivalence ratio, the upper bound of the stable range generally decreases with increasing pressure. The lower bound for an equivalance ratio of 0.9 corresponds closely to the lower ignition limits for the same equivalence ratio, as expected. The results of this study, which describe the range of stable reactant velocities, may not be applicable to another premixed flat-flame burner with a porous disk of a different diameter or thickness.

For calculating the reactant velocity in the burner mixing chamber, or burner cavity, the pressure in that cavity was estimated from nitrogen-flow—pressure-drop measurements of the porous disk in the burner. An error analysis of those measurements, based on a friction-factor—Reynolds number correlation for porous media, indicated that the pressure in the burner cavity, and hence the reactant velocity, could be in error by as much as 18 percent.

For the design of thermocouple probes, flame zone thickness and flame heights were measured from color photographs. Flame height is defined as the distance from the top of the porous disk to the bottom of the flame zone. Flame zone thicknesses ranged from 0.3 to 1.2 mm, and flame heights varied from 0.16 to 0.85 mm, which means that thermocouple probes should be on the order of 0.03 mm or smaller for good spatial resolution.

Langley Research Center
National Aeronautics and Space Administration
Hampton, VA 23665
September 28, 1978

APPENDIX A

EQUATIONS FOR CALCULATING REACTANT VELOCITY

Reactant velocity is the average axial velocity of the unburned gas in the burner mixing chamber. Reactant velocity was calculated from measured flow rates, pressure, and burner mixing-chamber temperature.

Thermal mass flowmeters were calibrated to measure flow rate at standard temperature (293 K) and pressure (1 atm). In effect, they measure the molar flow rate of a gas, for by the ideal gas law

$$nR = \frac{p_s V_s}{T_s} \tag{A1}$$

where n is the number of moles of gas, R is the universal gas constant, p_s is the absolute pressure at standard conditions, V_s is the volume of gas at standard conditions (1 atm, 293 K), and T_s is the absolute temperature at standard conditions. For a gas that acts ideal at low to moderate pressures and at moderate to high temperatures, which applies to methane and air at pressures up to 20 atm and at temperatures above 250 K,

$$nR = \frac{p_s V_s}{T_s} = \frac{pV}{T} \tag{A2}$$

where p is the pressure, V is the volume of gas at working pressure and temperature, and T is the absolute temperature. Differentiating equation (A2) with respect to time yields

$$\frac{\dot{pV}}{T} = \frac{p_s \dot{V}_s}{T_s} \tag{A3}$$

where $\dot{V}$ is the volumetric flow rate of unburned gas leaving the burner at pressure and temperature and $\dot{V}_s$ is the volumetric flow rate of unburned gas at standard conditions. Solving equation (A3) for $\dot{V}$, one gets

$$\dot{V} = \frac{p_s T}{p T_s} \dot{V}_s \tag{A4}$$

However, reactant velocity u_b is based on the volumetric flow rate inside the burner mixing chamber, or burner cavity $\dot{V}_b$. That is

$$u_b = \frac{\dot{V}_b}{A_b} \tag{A5}$$

where A_b is the cross-sectional area of the porous disk in the burner. Following the same reasoning in arriving at equation (A4),

$$\dot{V}_b = \frac{p_s T_b}{p_b T_s} \dot{V}_s \tag{A6}$$

where T_b and p_b are the absolute temperature and pressure in the burner cavity. T_b is determined from the temperature measured by the thermocouple probes in the burner cavity.

APPENDIX B

ERROR ESTIMATE IN PRESSURE OF BURNER CAVITY

The Kozeny-Carman equation for fluid friction in the flow through beds of solids (ref. 21) can be written as

$$p_1 - p_2 = \frac{L\rho\bar{u}^2(1 - \varepsilon)s_p}{\varepsilon^3 v_p} f \tag{B1}$$

where $p_1 - p_2$ is the pressure drop in the bed, L is the depth of the bed, ρ is the density of the fluid, $\bar{u}$ is the average velocity of the fluid based on the cross-sectional area of the empty conduit without the bed, ε is the void fraction or porosity, s_p and v_p are the surface area and volume of a single particle, and f is the friction factor. If the fluid is an ideal gas, then

$$\rho = \frac{M\bar{p}}{R\bar{T}} \tag{B2}$$

where M is the molecular weight of the gas, $\bar{p}$ is the average pressure of the gas in the bed, R is the universal gas constant, and $\bar{T}$ is the average absolute temperature of the gas in the bed. An expression for $\bar{u}$ is

$$\bar{u} = \frac{\dot{V}}{S} = \frac{\dot{V}_s \bar{T} p_s}{S T_s \bar{p}} \tag{B3}$$

where $\dot{V}$ is the volumetric flow rate of gas in the bed, S is the cross-sectional area of the bed, which is equal to A_b, the projected cross-sectional area of the burner, $\dot{V}_s$ is the volumetric flow rate of gas in the bed at standard conditions, and p_s and T_s are the absolute pressure and temperature (293 K) at standard conditions. Substituting equations (B2) and (B3) into equation (B1) and rearranging yields

$$p_1 - p_2 = \left[\frac{L(1 - \varepsilon)s_p p_s^2}{\varepsilon^3 R S^2 T_s^2 v_p}\right]\left[M\dot{V}_s^2\left(\frac{\bar{T}}{\bar{p}}\right)f\right] \tag{B4}$$

Let

$$\frac{L(1 - \varepsilon)s_p p_s^2}{\varepsilon^3 R S^2 T_s^2 v_p} = C \tag{B5}$$

where C is a constant since the values in this expression are either true constants or were constant for this study. With this expression, equation (B4) becomes

$$p_1 - p_2 = C\dot{M}V_s^2\left(\frac{\bar{T}}{\bar{p}}\right)f \tag{B6}$$

Solve for f to obtain

$$f = \frac{p_1 - p_2}{C\dot{M}V_s^2\left(\frac{\bar{T}}{\bar{p}}\right)} \tag{B7}$$

Also, from the Kozeny-Carman equation

$$f = F(N_{Re}) \tag{B8}$$

where

$$N_{Re} = \frac{\bar{u}\rho v_p}{\bar{\mu}s_p(1 - \varepsilon)} \tag{B9}$$

and $\bar{\mu}$ is the average viscosity of the gas in the bed. Substituting equations (B2) and (B3) into equation (B9) yields

$$N_{Re} = \left[\frac{v_p}{s_p(1 - \varepsilon)}\right]\left(\frac{p_s}{RST_s}\right)\frac{\dot{M}V_s}{\bar{\mu}} \tag{B10}$$

Let

$$\left[\frac{v_p}{s_p(1 - \varepsilon)}\right]\left(\frac{p_s}{RST_s}\right) = K \tag{B11}$$

K is a constant since all the values in this expression are either true constants or were constant for this study. With this expression, equation (B10) becomes

$$N_{Re} = K\frac{\dot{M}V_s}{\bar{\mu}} \tag{B12}$$

Thus, equation (B8) can be written as

$$f = F\left(K \frac{M\dot{V}_s}{\bar{\mu}}\right) \tag{B13}$$

The values of v_p and s_p in equation (B11) were calculated from a microscopic measurement of the spherical particles on the surface of the porous bronze disk. The value of ε in this equation was calculated from the ratio of the specific volume of bronze to the specific volume of the porous bronze disk, a value furnished by the manufacturer. The corresponding values of f and N_{Re} were calculated from equations (B7) and (B12) using the nitrogen-flow—pressure-drop data of figure 5 and plotted as shown in figure 14. For the range of N_{Re} from 1 to 10, the f values range from 10 to 100. These values of f are higher than those shown by McCabe and Smith (ref. 21) for the same range of N_{Re}; they show a range of f from 1 to 10.

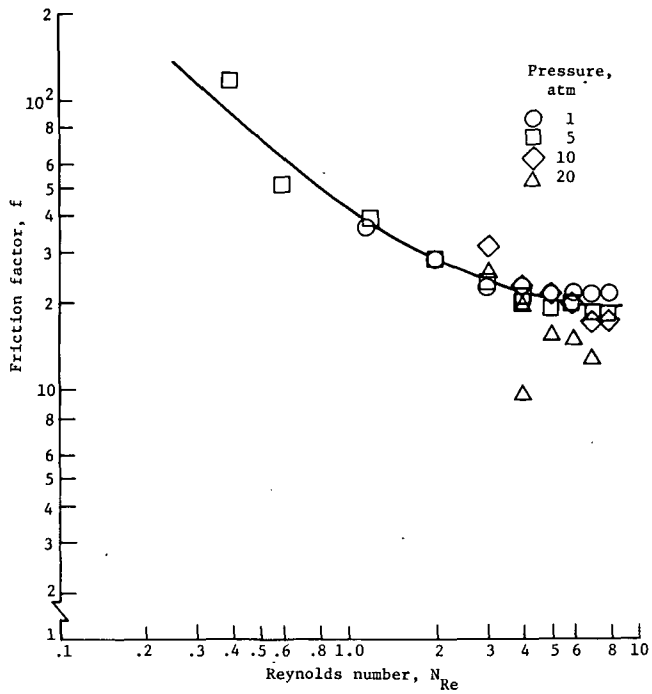

Figure 14.- Friction-factor—Reynolds number correlation for the nitrogen-flow—pressure-drop data.

The difference is probably because the values of reference 21 are based on Berl saddles or rings, a relatively open structure, and the data of this study are for a porous disk having a very closely packed structure of sintered spherical particles 0.13 mm in diameter. The curve of figure 14 should also apply to the methane-air reactant mixture.

Equation (B12) was then used to calculate N_{Re} for a range of $\dot{V}_s$ for the reactant mixture, with M taken at 28 g/mole for the reactants and $\bar{\mu}$ given by the equation

$$\bar{\mu} = \frac{\mu(T_1) + \mu(T_2)}{2} \tag{B14}$$

where $\mu(T_1)$ is the value of μ at the maximum measured temperature (350 K) in the burner cavity T_b, and $\mu(T_2)$ is the value of μ at an assumed temperature T_2 at the outlet of the porous disk. The two levels of T_2 assumed were 450 K and 550 K, which correspond to average temperatures in the porous disk of 400 K and 450 K, respectively. With these calculated values of N_{Re}, figure 14 was used to obtain the corresponding values of f. Then equation (B7) was used in the following form to calculate p_1, or p_b:

$$p_1^2 - p_2^2 = 2CM\dot{V}_s^2\bar{T}f \tag{B15}$$

with p_2 taken as 1 atm and $\bar{T}$ defined as

$$\bar{T} = \frac{T_1 + T_2}{2} \tag{B16}$$

The difference between this calculated value of p and the value of p_1 determined from the isothermal condition with nitrogen gas can be expressed as a percent error in p_1, as shown in figure 15.

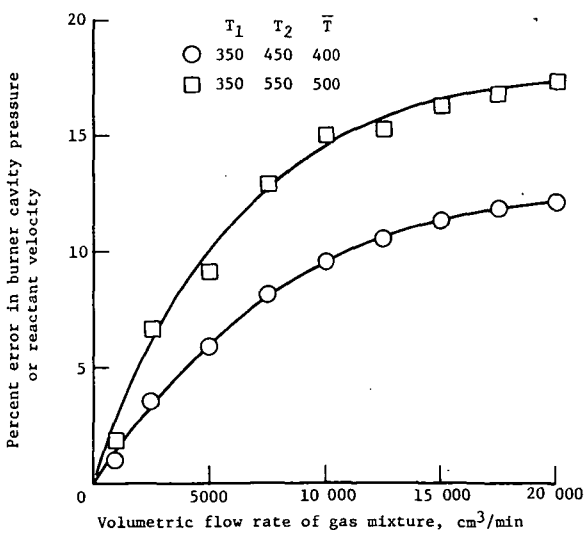

Figure 15.- Percent error in burner cavity pressure or reactant velocity as a function of volumetric flow rate of reactant gas under standard conditions for two assumed values of burner exit temperature T_2.

REFERENCES

1. Edse, Rudolph: Studies on Bunsen Burner Flames at High Pressures With Hydrogen-Oxygen Mixtures. Bull. No. 149, Eng. Exp. Stn., Ohio State Univ. Stud., Eng. Ser., 1952, pp. 441-457.

2. Diederichsen, J.; and Wolfhard, H. G.: Spectrographic Examination of Gaseous Flames at High Pressure. Proc. R. Soc. London, ser. A, vol. 236, no. 1204, July 10, 1956, pp. 89-103.

3. Diederichsen, J.; and Wolfhard, H. G.: The Burning Velocity of Methane Flames at High Pressure. Trans. Faraday Soc., vol. 52, pt. 8, no. 404, Aug. 1956, pp. 1102-1109.

4. Macfarlane, J. J.; Holderness, F. H.; and Whitcher, F. S. E.: Soot Formation Rates in Premixed C_5 and C_6 Hydrocarbon-Air Flames at Pressures up to 20 Atmospheres. Combust. & Flame, vol. 8, no. 3, Sept. 1964, pp. 215-229.

5. Strauss, William A.; and Edse, Rudolph: Investigation of Flames Burning at Pressures up to 100 Atmospheres. WADC Tech. Rep. 56-49, U.S. Air Force, June 1956.

6. Heberling, P. V.: "Prompt NO" Measurements at High Pressures. Sixteenth Symposium (International) on Combustion, Combustion Inst., 1976, pp. 159-168.

7. Miller, Irvin M.; and Maahs, Howard G.: High-Pressure Flame System for Pollution Studies With Results for Methane-Air Diffusion Flames. NASA TN D-8407, 1977.

8. Gaydon, A. G.; and Wolfhard, H. G.: Flames - Their Structure, Radiation and Temperature. Second ed., Rev. Chapman & Hall Ltd. (London), 1960, pp. 98-99.

9. Zabetakis, Michael G.: Safety With Cryogenic Fluids. Plenum Press, Inc., 1967, p. 57.

10. Barnett, Henry C.; and Hibbard, Robert R., eds.: Basic Considerations in the Combustion of Hydrocarbon Fuels With Air. NACA Rep. 1300, 1957, pp. 84-87.

11. Friedman, Raymond; and Johnston, W. C.: The Wall-Quenching of Laminar Propane Flames as a Function of Pressure, Temperature, and Air-Fuel Ratio. J. Appl. Phys., vol. 21, no. 8, Aug. 1950, pp. 791-795.

12. Friedman, Raymond; and Johnston, W. C.: Pressure Dependence of Quenching Distance of Normal Heptane, Iso-Octane, Benzene, and Ethyl Ether Flames. J. Chem. Phys., vol. 20, no. 5, May 1952, pp. 919-920.

13. Nair, M. R. S.; and Gupta, M. C.: Measurement of Flame Quenching Distances in Constant Volume Combustion Vessels. Combust. & Flame, vol. 21, no. 3, Dec. 1973, pp. 321-324.

14. Green, K. A.; and Agnew, J. T.: Quenching Distances of Propane-Air Flames in a Constant-Volume Bomb. Combust. & Flame, vol. 15, no. 2, Oct. 1970, pp. 189-191.

15. Von Elbe, Guenther; and Lewis, Bernard: Theory of Ignition, Quenching and Stabilization of Flames of Nonturbulent Gas Mixtures. Third Symposium on Combustion and Flame and Explosion Phenomena, Williams & Wilkins Co., 1949, pp. 68-79.

16. Lewis, Bernard; and Von Elbe, Guenther: Combustion, Flames and Explosions of Gases. Second ed. Academic Press, Inc., 1961, pp. 546-547.

17. Kihara, D. H.; Fox, J. S.; and Kinoshita, C. M.: Temperature and Velocity Non-Uniformity in Edge Cooled Flat Flame Burners. Combust. Sci. & Technol., vol. 11, no. 5-6, 1975, pp. 239-246.

18. Pritchard, Robert; Edmondson, Harry; and Heap, Michael Peter: Diameter Effects in Cooled-Flat-Flame Burners. Combust. & Flame, vol. 18, no. 1, Feb. 1972, pp. 13-18.

19. Spalding, D. B.; and Yumlu, V. S.: Experimental Demonstration of the Existence of Two Flame Speeds. Combust. & Flame, vol. 3, 1959, pp. 553-556.

20. Schlichting, Hermann (J. Kestin, transl.): Boundary-Layer Theory. Sixth ed. McGraw-Hill Book Co., 1968, pp. 560, 681.

21. McCabe, Warren L.; and Smith, Julian C.: Unit Operations of Chemical Engineering. McGraw-Hill Book Co., 1956, p. 95.

22. Botha, J. P.; and Spalding, D. B.: The Laminar Flame Speed of Propane/Air Mixtures With Heat Extraction From the Flame. Proc. R. Soc. London, ser. A, vol. 225, no. 1160, Aug. 6, 1954, pp. 71-96.

23. Bonne, U.; Grewer, Th.; and Wagner, H. Gg.: Messungen in der Reaktionszone von Wasserstoff—Sauerstoff-und Methan—Sauerstoff-Flammen. Z. Phys. Chem. (Neue Folge), Bd. 26, heft 1 and 2, 1960, pp. 93-110.

1. Report No.	2. Government Accession No.	3. Recipient's Catalog No.
NASA TP-1318		

4. Title and Subtitle	5. Report Date
A HIGH-PRESSURE PREMIXED FLAT-FLAME BURNER FOR CHEMICAL PROCESS STUDIES	December 1978
	6. Performing Organization Code

7. Author(s)	8. Performing Organization Report No.
Irvin M. Miller	L-12347
	10. Work Unit No.
	505-03-23-01

9. Performing Organization Name and Address	11. Contract or Grant No.
NASA Langley Research Center Hampton, VA 23665	
	13. Type of Report and Period Covered
	Technical Paper

12. Sponsoring Agency Name and Address	14. Sponsoring Agency Code
National Aeronautics and Space Administration Washington, DC 20546	

15. Supplementary Notes

16. Abstract

A premixed flat-flame burner was designed and tested with methane-air mixtures at pressures from 1.1 to 20 atm and equivalence ratios from 0.7 to 1.1. Reactant velocity in the burner mixing chamber was used to characterize the range of stable flames at each pressure—equivalence-ratio condition. Color photographs of the flames were used to determine flame zone thickness and flame height. The results show that this burner can be used for chemical process studies in premixed high-pressure methane-air flames up to 20 atm.

17. Key Words (Suggested by Author(s))	18. Distribution Statement
Premixed flames Burners Air pollution Methane High pressure	Unclassified - Unlimited Subject Category 25

19. Security Classif. (of this report)	20. Security Classif. (of this page)	21. No. of Pages	22. Price*
Unclassified	Unclassified	28	$4.50

* For sale by the National Technical Information Service, Springfield, Virginia 22161

National Aeronautics and
Space Administration

Washington, D.C.
20546

Official Business
Penalty for Private Use, $300

THIRD-CLASS BULK RATE

Postage and Fees Paid
National Aeronautics and
Space Administration
NASA-451

NASA

POSTMASTER: If Undeliverable (Section 158 Postal Manual) Do Not Return